Accepted Manuscript

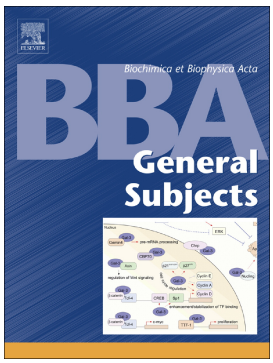

Increased intracellular iron in mouse primary hepatocytes in vitro causes activation of the Akt pathway but decreases its response to insulin

Joe Varghese, Jithu James, Sophie Vaulont, Andrew Mckie, Molly Jacob

PII: S0304-4165(18)30154-5
DOI: doi:10.1016/j.bbagen.2018.05.022
Reference: BBAGEN 29128

To appear in: *BBA - General Subjects*

Received date: 8 January 2018
Revised date: 17 May 2018
Accepted date: 28 May 2018

Please cite this article as: Joe Varghese, Jithu James, Sophie Vaulont, Andrew Mckie, Molly Jacob , Increased intracellular iron in mouse primary hepatocytes in vitro causes activation of the Akt pathway but decreases its response to insulin. Bbagen (2018), doi:10.1016/j.bbagen.2018.05.022

Increased intracellular iron in mouse primary hepatocytes *in vitro* causes activation of the Akt pathway but decreases its response to insulin

Joe Varghese[1,4,5], Jithu James[1,4], Sophie Vaulont[2], Andrew Mckie[3], Molly Jacob[1]

[1] Department of Biochemistry, Christian Medical College*, Vellore -632002, India

[2] INSERM U1016, Paris, France

[3] Diabetes and Nutritional Sciences Division, School of Medicine, King's College, London, UK

[4] Co-first authors

[5] Corresponding author

Corresponding author:

Dr. Joe Varghese

Department of Biochemistry

Christian Medical College, Vellore

Tamil Nadu, India – 632002

Tel: +91-416-2284267

E-mail: joevarghese@cmcvellore.ac.in

***** affiliated to The Tamil Nadu Dr. M.G.R. Medical University, Chennai, India.

Abstract

Background

An iron-overloaded state has been reported to be associated with insulin resistance. On the other hand, conditions such as classical hemochromatosis (where iron overload occurs primarily in the liver) have been reported to be associated with increased insulin sensitivity. The reasons for these contradictory findings are unclear. In this context, the effects of increased intracellular iron *per se* on insulin signaling in hepatocytes are not known.

Methods

Mouse primary hepatocytes were loaded with iron *in vitro* by incubation with ferric ammonium citrate (FAC). Intracellular events related to insulin signaling, as well as changes in gene expression and hepatocyte glucose production (HGP), were studied in the presence and absence of insulin and/or forskolin (a glucagon mimetic).

Results:

In vitro iron-loading of hepatocytes resulted in phosphorylation-mediated activation of Akt and AMP-activated protein kinase. This was associated with decreased basal and forskolin-stimulated HGP. Iron attenuated forskolin-mediated induction of the key gluconeogenic enzyme, glucose-6-phosphatase. It also attenuated activation of the Akt pathway in response to insulin, which was associated with decreased protein levels of insulin receptor substrates 1 and 2, constituting insulin resistance.

Conclusions

Increased intracellular iron has dual effects on insulin sensitivity in hepatocytes. It increased basal activation of the Akt pathway, but decreased activation of this pathway in response to insulin.

General significance

These findings may help explain why both insulin resistance and increased sensitivity have been observed in iron-overloaded states. They are of relevance to a variety of disease conditions characterized by hepatic iron overload and increased risk of diabetes.

Keywords: iron; insulin resistance; Akt; gluconeogenesis; diabetes mellitus; hemochromatosis

List of abbreviations:

ACC (acetyl CoA carboxylase), Akt (acute transforming retrovirus thymoma), AMPK (5'-adenosine monophosphate-activated protein kinase), AMPKK (AMPK kinase), BCA (bicinchoninic acid), DFO (desferrioxamine), FAC (ferric ammonium citrate), FoxO1 (forkhead box protein O1), Gsk3β (glycogen synthase kinase 3β), Hamp1 (hepcidin anti-microbial peptide), IR (insulin resistance), IRS (insulin receptor substrate), JNK (c-Jun N-terminal kinase), LKB1 (liver kinase B1), mTOR (mechanistic target of rapamycin), PFKFP (phosphofructokinase-2/fructose bisphophatase-2), PGC1α (peroxisome proliferator-activated receptor gamma coactivator 1-alpha), PVDF (polyvinylidene fluoride), SPSS (Statistical Package for the Social Sciences), TfR1 (transferrin receptor 1).

1. Introduction

Insulin resistance (IR) is the hallmark of type 2 diabetes mellitus (T2DM). Several lines of evidence suggest that iron plays a role in the pathogenesis of IR [1]. For example, children with thalassemia major, who are treated with repeated blood transfusions and have increased body iron stores, develop hyperinsulinemia and IR before they develop diabetes [2]. Aggressive iron chelation has reduced the incidence of diabetes in patients with thalassemia [3]. Further evidence for the role of iron in IR is provided by improvements in insulin sensitivity following phlebotomy, both in patients with T2DM [4] and in healthy individuals [5]. Iron-deficient rats show increased peripheral glucose uptake in response to insulin [6,7]. Phlebotomy or dietary iron restriction, in a rat model of T2DM, resulted in decreased glycated hemoglobin levels [8]. Iron chelation significantly protected *ob/ob* mice from diabetes [9] and improved insulin signaling in the rat liver [10]. On the other hand, mice fed a high-iron diet have been shown to develop insulin resistance [11].

Increased hepatic glucose production (HGP), driven primarily by increased gluconeogenesis, is a characteristic feature of diabetes [12]. Regulation of HGP is a complex process, with glucagon and insulin being the primary hormonal regulators [13]. Glucagon stimulates HGP by activating (via phosphorylation) the bi-functional enzyme, phosphofructokinase-2/fructose bisphophatase-2, thus increasing the gluconeogenic flux [14,15]. It also increases the transcription of key gluconeogenic genes, phosphoenolpyruvate carboxykinase (PEPCK, *Pck1)* and glucose-6-phosphatase *(G6pc)*, by activating the transcription factor, cAMP-response element binding protein (CREB) [16]. While glucagon sets the basal tone for HGP, insulin can powerfully suppress it by acting through multiple mechanisms [17]. Insulin, acting via its receptor on the cell surface, phosphorylates and activates Akt (protein kinase B) [18]. Activated Akt

phosphorylates several downstream targets, including glycogen synthase kinase 3β (Gsk3β) (at Ser9) and forkhead box O1 (FoxO1) (at Ser256), causing inactivation of both. Inactivation of Gsk3β inhibits glycogenolysis, while that of FoxO1 results in suppression of gluconeogenesis [19]. In addition to transcriptional regulation of hepatic gluconeogenic genes, it is now known that insulin can robustly suppress HGP in mice by acting indirectly, through inhibition of lipolysis in the adipose tissue [20].

AMP-activated protein kinase (AMPK) is a key cellular energy sensor that is activated in response to a multitude of stimuli [21]. AMPK activation results in inhibition of anabolic pathways (which consume ATP) and stimulation of catabolic pathways (which increase ATP production). AMPK is known to decrease HGP by inducing the phosphorylation and inactivation of CREB-regulated transcription co-activator 2 (CRTC2), a key transcriptional co-activator involved in induction of gluconeogenic genes by glucagon [22]. In addition, AMPK also inhibits glucagon-induced increase in gluconeogenesis, by activating phosphodiesterase-mediated cAMP degradation [23].

Hereditary hemochromatosis comprises a group of conditions characterized by increased body iron stores, which results from inappropriately low levels of hepcidin, the central iron regulatory hormone [24]. Although raised iron stores are associated with IR (as described above), other studies have shown that insulin sensitivity was increased in patients with classical hemochromatosis and in mouse models of the condition (*Hfe*$^{-/-}$ mice) [25,26]. The reason(s) for these apparently contradictory findings are not clear; they may be related to the fact that, in hemochromatosis, iron accumulates to a greater extent in the liver [27] compared to other tissues, such as skeletal muscle and adipose tissue [28]. Such differences in iron levels in tissues may potentially affect results from studies done in humans and animal models of hemochromatosis, as

glucose tolerance *in vivo* is determined by factors that regulate insulin sensitivity in both the liver and peripheral tissues. For example, insulin has been shown to suppress HGP indirectly by inhibiting lipolysis in adipose tissue and not only by acting directly on the liver [20]. In this context, the effect of increased levels of iron *per se* on hepatic insulin signaling and HGP is unclear. Similarly, it has been shown that, in mice fed a high-iron diet, AMPK is activated in the liver and skeletal muscle; this was associated with decreased HGP [29]. However, it is not known whether the decrease in HGP in this context was a direct effect of increased levels of hepatic iron or mediated by the effects of iron overload in non-hepatic tissues.

In the present study, the effects of high intracellular iron levels on insulin signaling and HGP in mouse primary hepatocytes were determined. These effects were studied *in vitro* in order to avoid confounding factors that are operational *in vivo* that would influence the effects that we were interested in studying.

2. Methods

2.1. Animals

Male C57Bl/6 mice, aged between 10 and 12 weeks, were used for all the experiments. These were carried out with the approval of the Institutional Animal Ethics Committee at Christian Medical College, Vellore, India (IAEC No. 8/2014), in accordance with the regulations of the Committee for the Purpose of Control and Supervision of Experiments on Animals (CPCSEA), Government of India.

2.2. Isolation of mouse primary hepatocytes

Mouse primary hepatocytes were isolated using a modified collagenase perfusion method, as described earlier [30] (see Supplementary Methods for details). Viability of the isolated cells (as determined by trypan blue exclusion) was consistently found to be more than 85%. The cells were seeded in 6- or 12-well collagen-coated plates at a density of 5 x 10^4 cells per cm^2, in DMEM with 10% fetal calf serum, and allowed to adhere to the bottom of the wells for 2 hours.

2.3. Treatment of hepatocytes with iron and/or insulin

Two hours after seeding, cells were washed with PBS and maintained in serum-free DMEM, which was supplemented with ferric ammonium citrate (FAC) at 0, 7.5, 75 or 750 μM concentrations for 16 hours (in order to increase the intracellular iron content) [31]. Primary hepatocytes were maintained in serum-free DMEM because it is known that serum has an inhibitory effect on expression of liver-specific proteins in isolated hepatocytes [32,33]. To study the effects of insulin on control or FAC-treated hepatocytes, cells were washed with PBS and then treated with insulin (10 nM) for 5 minutes (for study of intracellular signaling events) or 3 hours (for gene expression studies). A concentration of 10 nM of insulin was chosen because this is a concentration that has been commonly used in studies that have assessed insulin signaling in primary hepatocytes [34–36]. In addition, our preliminary experiments showed that insulin-induced activation of Akt (phosphorylation at Ser473) was similar at 10 and 100 nM concentrations (data not shown). In a sub-set of hepatocytes treated with FAC (75 μM) for 16 hours, the cells were washed at the end of the incubation and then incubated with desferrioxamine (DFO) (250 μM) for 6 hours, in order to chelate iron.

2.4. Determination of cell viability

At the end of the incubations with FAC, the viability of the cells was determined by the MTT assay, estimation of lactate dehydrogenase (LDH) activity in the medium and by staining with ethidium homodimer-1 (EthD-1) (see Supplementary Methods for details).

2.5. Calcein fluorescence quenching by intracellular labile iron

Intracellular labile iron quenches calcein fluorescence [37] and a decrease in green fluorescence indicates increased intracellular labile iron. After treatment with or without FAC, cells were washed twice with PBS and incubated with calcein-AM (2 μM final concentration) for 30 min. Fluorescence was visualized under a fluorescence microscope using the standard fluorescein filter (see Supplementary Methods for details).

2.6. Hepatocyte glucose production assay

Hepatocyte glucose production assays were carried out as described earlier [30] (see Supplementary Methods for details). Briefly, hepatocytes treated with or without FAC were washed and incubated in glucose production buffer (glucose-free, phenol red-free DMEM supplemented with lactate [20 mM] or glycerol [10 mM] as the gluconeogenic substrate) for 3, 6, 9 or 12 hours. At the end of each time point, an aliquot of the medium was taken for estimation of glucose by the glucose oxidase-peroxidase (GOD-POD) method.

2.7. Quantitative real-time PCR (qPCR)

Quantitative real-time RT-PCR was used to determine the mRNA expression of genes of interest (see Supplementary Methods for details). Lysates were prepared from FAC- treated cells or control cells and total RNA was isolated using Tri-reagent (Sigma) following standard protocols.

The quality of the RNA isolated was ascertained and found to be consistently high. Sequences of all primers used are listed in Supplementary Table 1. Expression levels of genes of interest were normalized to that of Rpl19 which was used as the reference gene. MIQE check-list and qPCR primer validation data are provided in Supplementary Tables 3 and 4 respectively.

2.8. Western blotting

FAC-treated and control primary hepatocytes were homogenized in RIPA buffer and processed for western blotting, as described earlier [38] (see Supplementary Methods for details). Sources and dilutions of primary and secondary antibodies used are listed in Supplementary Table 2.

2.9. Iron estimation

Iron content in the FAC-treated and control hepatocytes was measured by a spectrophotometric assay, as described previously [39] (see Supplementary Methods for details).

2.10 Glucose-6-phosphatase enzyme assay

Enzyme activity of glucose-6-phosphatase (G6Pase) was estimated as described earlier [40] (see Supplementary Methods for details). Briefly, microsomal fractions were isolated from primary hepatocytes grown in 6-well plates, by differential centrifugation. G6Pase activity was estimated by incubating microsomal isolates with the substrate, glucose-6-phosphate (at a final concentration of 20 mM), at 30°C for 15 min (pH 6.5). The phosphate released was estimated by the method of Taussky and Shorr [41]. One unit of enzyme activity was defined as the amount of enzyme that releases 1 μmole of phosphate in one minute. Non-specific hydrolysis of glucose-6-phosphate, by phosphatases other than G6Pase, was determined by estimation of phosphate released when beta-glycerophosphate was used as the substrate (beta-glycerophosphate is not a

substrate for G6Pase [42]). Results were corrected for non-specific phosphatase activity and normalized to microsomal protein content in each sample.

2.11. Statistical analyses

Statistical Package for Social Scientists (SPSS), version 16.0, was used for all statistical analyses. The Kruskal-Wallis test was used to look for effects of the various treatments on the parameters of interest. Pair-wise comparisons were done using the Mann-Whitney test. Correlation analysis was done by Spearman's correlation test. A p value of less than 0.05 was used to indicate statistical significance in all cases. Data was obtained from at least three independent experiments (primary hepatocytes isolated from at least 3 different mice), with each incubation done in duplicates or triplicates, under the specified conditions.

3. Results

3.1. Treatment of hepatocytes with FAC increased intracellular iron content

Primary hepatocytes treated with FAC, showed increases in cellular iron content (Fig. 1A). This was associated with increased protein levels of ferritin (Fig. 1B) and decreased levels of transferrin receptor 1 (TfR1) (Fig. 1 C). Intracellular labile iron quenches calcein fluorescence and the degree of quenching is indicative of the intracellular labile iron pool (LIP) [37]. By fluorescence microscopic imaging, a decrease in calcein fluorescence was found in hepatocytes treated with FAC, indicating an increase in the LIP (Fig. 1D). These results show that FAC treatment resulted in an increase in intracellular iron with a concomitant increase in the LIP.

Treatment of hepatocytes with iron did not affect cell viability, as determined by the MTT assay (Fig. 1E). However, there was a small but significant increase in LDH activity in the medium, at

the highest dose of FAC used (750 μM) (Fig. 1F). Similarly, fluorescence microscopic imaging of cells stained with ethidium homodimer-1 (EthD-1), showed a marginal increase in red fluorescence in cells treated with 750 μM FAC (Suppl. Fig. 1). There was, however, no change in cells treated with 7.5 and 75 μM FAC compared to untreated cells. Treatment of hepatocytes with iron induced hepcidin (*Hamp1*) expression (Suppl Fig 2A). Iron did not affect the mRNA expression of the acute-phase proteins, C-reactive protein (*Crp)* (Suppl Fig 2B) and serum amyloid A1 protein (*Saa1*) (Suppl Fig 2C), and the pro-inflammatory cytokine, interleukin- 6 (*Il6*) (Suppl Fig 2D). However, iron induced the expression of tumor necrosis factor alpha (*Tnfa*) (at both 7.5 and 75 μM) (Suppl Fig 2E). Iron also induced the expression of heme oxygenase–1 (*Hmox1*) (Suppl Fig 2F) and a small, but statistically significant, increase in the expression of *Cyba* (p22-phox subunit of NADPH oxidase) (Suppl Fig 2G), suggesting the presence of oxidative stress in this setting.

3.2. Treatment with iron increased phosphorylation of Akt and its downstream targets, Gsk3β and FoxO1

Activation of Akt involves phosphorylation at Thr308 and Ser473 [18]. FAC treatment resulted in increases in phosphorylation of Akt at both Thr308 and Ser473, without affecting total Akt levels (Fig. 2A and B). Increased phosphorylation of downstream targets of activated Akt, viz. Gsk3β (Fig. 2C) and FoxO1 (Fig. 2D), was also seen. Treatment of hepatocytes with DFO (250 μM) (an iron chelator) for 6 hours after pre-treatment with FAC (for 16 hours) resulted in significant decreases in intracellular iron content (Fig. 2E) and was associated with attenuation of iron-induced Akt phosphorylation (Fig. 2F).

3.3. Treatment with iron activated AMP-activated kinase (AMPK)

Since AMPK activation has been shown to trigger the phosphorylation and activation of Akt and GSK3β in the liver [43], the effect of iron on AMPK was examined in the current study. Treatment with FAC induced an increase in the phosphorylation of AMPK at Thr172 (Fig. 3A). The downstream target of AMPK, acetyl CoA carboxylase (ACC), was also found to be phosphorylated at Ser79 (Fig. 3A; lower panel). Activated AMPK is known to phosphorylate and inhibit sterol response element-binding protein 1c (SREBP-1c), resulting in suppression of lipogenesis, by decreasing mRNA levels of ACC (*Acaca*) and fatty acid synthase (*Fasn*) [44,45]. In addition, SREBP-1c inhibition has been shown to result in induction of *Irs2* but not of *Irs 1* [46]. In keeping with these reported effects, treatment with FAC was found to reduce mRNA expression of *Acaca* and *Fasn*, and increase the expression of *Irs2* (Fig. 3B, C and D); no significant changes were seen in *Irs1* expression (Fig. 3E).

3.4. Treatment with iron decreased hepatocyte glucose production (HGP)

In order to assess the functional consequences of activation of the Akt and AMPK pathways by iron, we measured hepatocyte glucose production (HGP), both in the presence and absence of FAC, using lactate and glycerol as gluconeogenic substrates. We used FAC at concentrations of 7.5 μM and 75 μM for these measurements, avoiding the concentration of 750 μM at which some extent of cell damage was observed (Fig 1F and Suppl Fig 1). Hepatocytes treated with FAC at 75 μM showed significantly lower HGP, when compared to control cells or those treated with FAC 7.5 μM; the effects seen were similar irrespective of the use of lactate or glycerol as the gluconeogenic substrate (Fig 4A and C). At 7.5 μM, FAC tended to lower glucose production, when compared to control cells, but the effects were not statistically significant except at 3 and 6 h (in the case of lactate-driven basal HGP) (Fig. 4A). Forskolin, an adenylyl cyclase activator

that mimics the effects glucagon in hepatocytes [47], was used to induce HGP. Forskolin-induced HGP was significantly attenuated by FAC (75 μM) treatment (Fig 4B and D). These results show that iron significantly decreased both basal and forskolin-induced HGP in hepatocytes. Treatment with insulin, on the other hand, did not have an effect on HGP, neither in the presence of forskolin nor in its absence (Suppl Fig 3)

Since similar changes in HGP were found irrespective of lactate or glycerol being used as the gluconeogenic substrate, effects of iron on gene expression and activity of glucose-6-phosphatase (G6Pase) (an enzyme involved in gluconeogenesis from both of these substrates) was determined. Treatment of hepatocytes with FAC at 7.5 μM did not produce any significant effect on G6Pase mRNA levels; treatment with 75 μM of FAC a small but significant increase in levels (Fig. 4E). However, activity of G6Pase was lower in hepatocytes treated with FAC, with a concentration-dependent effect seen, but the decreases were not statistically significant (Fig. 4F). Prior treatment of hepatocytes with FAC attenuated forskolin-induced increases in G6Pase mRNA (Fig. 4E) and activity (Fig. 4F), with the attenuation being more marked with increasing concentrations of iron. Iron also attenuated insulin-induced suppression of G6Pase mRNA (Fig. 5C). A similar pattern was observed in G6Pase activity as well (though the effects were not statistically significant) (Fig. 5D).

3.5. Treatment with iron rendered hepatocytes less sensitive to insulin-induced activation of the Akt pathway

In order to assess the effect of iron on insulin-induced activation of the Akt pathway, hepatocytes were incubated with different doses of FAC for 16 h followed by treatment for 5 min with insulin (10 nM). Insulin-induced activation of Akt (Fig. 5A), as well as Gsk3β (Fig 5B) (the

downstream target of activated Akt), was significantly attenuated by treatment with iron. In keeping with this observation, insulin was found to neither suppress *G6pc* (Fig. 5C) nor induce glucokinase (*Gck)* (Fig. 5E) in FAC-treated hepatocytes. Both of these are known responses to insulin and were observed in the current study in the absence of FAC treatment (Fig. 5C and E). These results suggest that increased intracellular iron rendered hepatocytes resistant to the effects of insulin.

3.6. Iron down-regulated protein levels of IRS1 and IRS2

Insulin receptor substrates 1 and 2 (IRS 1 and 2) are upstream of Akt in the insulin signaling pathway. With increasing concentration of FAC, protein levels of IRS1 and IRS2 decreased (Fig. 6A and B). Phosphorylation of IRS1 at Ser307 (Fig. 6C) and Ser789 (Fig. 6D), both of which are known to inhibit signaling via IRS-1, tended to increase progressively in response to increasing concentrations of FAC, but the increases were statistically significant only at 750 μM FAC. There was also no demonstrable activation of JNK (c-Jun N-terminal kinase), a stress-induced kinase known to phosphorylate IRS1 at Ser307 (Fig. 6F).

3.7 Correlational analyses

Results of correlation analyses showed that, in FAC-treated hepatocytes, intracellular iron levels were significantly and positively correlated with p-Akt (Ser473), p-Akt (Thr308), p-Gsk3β (Ser9), p-FoxO1 (Ser256) and p-AMPK (Thr172), and negatively correlated with IRS1 and IRS2 protein levels. In addition, markers of insulin signaling (p-Akt [Ser473], p-Akt [Thr308], p-Gsk [Ser9] and p-FoxO1 [Ser256]) were significantly and positively correlated with one another and with p-AMPK (Thr172) (Table 1).

4. Discussion

Molecular interactions between insulin signaling and iron in hepatocytes, and their effects on HGP have not been clearly elucidated. In order to study this, we used mouse primary hepatocytes, which were iron-loaded *in vitro* by incubation with FAC at various concentrations. *In vitro* systems do have limitations; however, in this context, this was the most appropriate model to use to answer the research question concerned, since we wished to avoid confounding factors that are operational *in vivo* (as described in the introduction section). The rationale for treating hepatocytes with FAC (a highly soluble form of iron) was to increase intracellular iron content. The doses of FAC chosen were based on a previous publication where primary hepatocytes treated with similar doses of FAC showed no decrease in cell viability [31]. In addition, FAC was chosen because ferric citrate is a physiologically relevant form of iron. It has been shown that non-transferrin bound iron (NTBI), which increases in blood in conditions of iron overload, such as hemochromatosis and thalassemia, is mainly found complexed with citrate [48,49].

Treatment of hepatocytes with FAC resulted in increases in intracellular iron content (Fig. 1 A-C). Although MTT assay showed no significant decrease in cell viability (Fig. 1D), there was a small but significant increase in LDH activity in the medium (Fig. 1 E) and increased EthD-1fluorescence (Suppl. Fig. 1) at the highest dose of FAC used (750 µM). This showed that FAC, at this dose, induced cell damage to a certain extent. However, all the effects of interest produced by treatment with FAC, which are reported in this study, were seen at 7.5 and 75 µM concentrations. No decrease in cell viability was seen at these doses.

The results of our study are summarized in Fig 7. Overall, the results showed that increases in intracellular iron had a dual effect on hepatocytes, with regard to the pathway of insulin signaling. On one hand, iron activated the Akt signaling pathway in hepatocytes in a ligand-independent manner, i.e., even in the absence of insulin (Fig. 2). In addition, iron activated AMPK, a key energy-sensing pathway (Fig. 3). Consequently, gluconeogenesis was down-regulated and HGP was decreased (Fig. 4). On the other hand, iron attenuated activation of the Akt pathway in response to insulin (Fig. 5); this was associated with decreased levels of IRS 1 and 2 (Fig. 6), thereby resulting in a state of insulin resistance. The findings of this study provide a plausible explanation for why iron overload, in general, is associated with insulin resistance (1–11) but improved glucose tolerance and insulin sensitivity is seen in classical hemochromatosis (which is characterized by iron overload primarily in the liver) [25,26]. To the best of our knowledge, our findings, in primary hepatocytes, are novel and have not been reported earlier.

AMPK is activated by its upstream kinase, liver kinase B1 (LKB1), by phosphorylation at Thr172 [21]. It has been shown previously that LKB1 and AMPK were activated in the liver and skeletal muscle of mice fed a high-iron diet [29]. Ligand-independent activation of the Akt pathway has been shown to occur in response to activation of AMPK [50,51], thus suggesting a likely mechanism by which Akt phosphorylation is induced by iron. FAC treatment resulted in activation of AMPK, which was highly significantly correlated with phosphorylation of Akt at both Thr308 and Ser473 (Table 1). It is, therefore, possible that iron-induced activation of Akt may be mediated by AMPK activation. Additional studies, utilizing techniques of gene knock-down and pharmacological inhibition of AMPK, would be required to confirm this.

It has been shown that di-2-pyridylketone 4,4-dimethyl-3-thiosemicarbazone (Dp44mT), a novel iron and copper chelator that has been shown to have anti-cancer activity, increases AMPK

activity in various cancer cell lines [52]. This is in contrast to the results of the present study where we have shown activation of AMPK in response to an increase in intracellular iron (Fig 3A). The exact mechanisms that underlie metal-ion chelation-induced activation of AMPK have not been clearly elucidated; however, there are several possible mechanisms. Both iron and copper are critical for mitochondrial electron transport chain [53]. Chelation of iron and copper by Dp44mT can therefore inhibit oxidative phosphorylation resulting in accumulation of AMP, which is a potent activator of AMPK [21]. Dp44mT is also known to generate ROS and induce oxidative stress in cells [52]; oxidative stress is known to activate AMPK [21].

Iron decreased basal as well as forskolin-induced HGP (Fig. 4A to D). It also attenuated forskolin-induced increases in mRNA expression of *G6pc* (Fig. 4E). Activation of the Akt pathway results in suppression of gluconeogenesis by inhibiting FoxO1-induced expression of *G6pc* [54,55]. Activation of AMPK has also been shown to decrease HGP by inducing the phosphorylation and inactivation of CRTC2, a key transcriptional co-activator involved in induction of gluconeogenic genes by glucagon [22]. In addition, AMPK inhibits glucagon-induced increase in *G6pc* expression by activating phosphodiesterase-mediated cAMP degradation [23]. Therefore, iron-induced activation of Akt and AMPK pathways can explain the decrease in HGP and *G6pc* expression in this setting.

The rate of glucose uptake by hepatocytes is chiefly regulated by glucokinase (GK) [56]. Insulin increases hepatocyte glucose uptake by increasing transcription of the gene for glucokinase (*Gck*) [57]. Consistent with this, our data shows that insulin induced mRNA expression of *Gck*; however, in the presence of iron, this effect was attenuated, while treatment of the cells with only iron did not affect *Gck* mRNA levels (Fig 5E). This tends to suggest that glucose uptake may not be affected in hepatocytes treated with iron. We attempted to estimate glucose uptake in

hepatocytes in this setting using a 2-deoxyglucose (2-DG) uptake assay (Cosmo Bio, Japan). However, we were unable to obtain reliable estimates of 2-DG uptake in hepatocytes due to high background signal obtained in the negative controls (hepatocytes not treated with 2-DG). This is a limitation of the present study.

Decreased HGP was seen in response to iron but was not associated with a corresponding decrease in expression of *G6pc*. In fact, iron (at 75 μM, but not at 7.5 μM) induced a small but significant increase in the mRNA levels of this enzyme (Fig. 4E). The reasons for decreased HGP in response to iron treatment are currently unclear. HGP is known to be regulated by post-translational mechanisms through the control of substrate flux, rather than exclusively by changes in gene expression [13]. We, therefore, estimated G6Pase enzyme activity in hepatocytes treated with iron. Activity of this enzyme was not affected by FAC treatment (Fig 4F). This seems to suggest that the inhibitory effect of iron on HGP is possibly not mediated by post-translational effects of iron on G6Pase enzyme activity.

The bi-functional enzyme, phosphofructokinase-2 /fructose–2,6–bisphosphatase (PFKFB), is a key enzyme involved in the reciprocal regulation of glycolysis and gluconeogenesis [58]. Insulin, by acting via the Akt pathway, can activate PFKFB (by de-phosphorylation), thus stimulating glycolysis and inhibiting gluconeogenesis. On the other hand, glucagon, acting via the second messenger cAMP, inactivates PFKFB (by phosphorylation) and has the opposite effect [59]. It is possible that iron-induced activation of the Akt pathway may underlie the decrease in HGP seen in this setting. In addition, activation of AMPK is known to decrease HGP by antagonizing glucagon signaling via phosphodiesterase-mediated degradation of cAMP [23]. Further work would be required to investigate these possibilities. A possible explanation for the increase in *G6pc* expression induced by FAC treatment (at 75 μM) (Fig 4E) may be iron-induced

mitochondrial dysfunction, which has been shown to occur in response to iron overload and result in increased expression of gluconeogenic genes [60].

Although treatment with iron activated the Akt pathway, activation of Akt (and its downstream target, GSK3β) in response to insulin treatment was significantly attenuated in iron-loaded hepatocytes (Fig 5A and B), suggesting that an iron-overloaded state results in resistance to the actions of insulin. We attempted to elucidate the functional consequences of this observation by studying HGP changes in response to insulin treatment. However, we found that insulin did not have an effect on HGP, neither in the presence of forskolin nor in its absence (Suppl Fig 3). This is consistent with recent studies which have shown that direct insulin signaling in hepatocytes is dispensable for insulin-mediated down-regulation of HGP [20,61]. Regulation of HGP by insulin *in vivo* has been suggested to be mediated by an intermediate extra-hepatic organ/tissue; this is most probably the adipose tissue, via changes in free fatty acid levels in blood [62].

In the present study, iron induced a progressive decrease in IRS1 and IRS2 protein levels (Fig. 6A and B). Since IRS1 and IRS2 are up-stream of Akt in the insulin signaling cascade, a decrease in the levels of these proteins could account for the impaired phosphorylation and decreased activation of Akt induced by insulin in these cells. Phosphorylation of IRS1 at Ser307 and its subsequent degradation has been proposed to play a key role in the development of insulin resistance [63]. Stress-induced protein kinases, including JNK and mTOR, are known to increase phosphorylation of IRS1 at Ser307 [64,65]. Our findings show that treatment with iron induced an increase in the p-IRS1 (Ser307)/total IRS1 ratio (Fig. 6C), but did not activate JNK (Fig. 6E). It is possible that increased phosphorylation of IRS1 at Ser307 in this setting could be mediated by mTOR; however, this possibility requires further exploration. In addition, iron

increased IRS1 phosphorylation at Ser789 (Fig. 6D). Phosphorylation of IRS-1 at Ser789 is known to be induced by AMPK [50] and inhibits signal transduction via IRS1 [66].

We found that treatment with iron induced the expression of TNF-alpha in isolated hepatocytes (Suppl Fig 2E). It has been previously shown that chronic iron loading (by administration of iron-dextran) in rats resulted in induction of TNF-alpha, but not of other cytokines, such as IL-6 and TGF-alpha, in the liver [67]. On the other hand, human primary hepatocytes, treated with holo-transferrin, showed induction of both TNF-alpha as well as IL-6 [68]. Additional studies would be required to elucidate the mechanisms that underlie the induction of TNF alpha by iron, and its pathophysiological significance, if any.

Findings of increased basal but decreased insulin-stimulated activation of Akt have been reported previously to result in insulin resistance. For example, it has been shown that overexpression of a constitutively active form of Akt increased basal glucose uptake, but blunted insulin-induced glucose uptake in cardiomyocytes [69]. Similarly, cardiomyocytes that over-expressed FoxO1, showed elevated basal, but impaired insulin-stimulated Akt phosphorylation and downstream insulin signaling [70]. *Hfe*$^{-/-}$ mice, that represent a model of hemochromatosis, also show increased basal, but not insulin-stimulated glucose uptake in the skeletal muscle [25]. Impaired activation of Akt in response to insulin treatment has also been shown in AML-2 mouse hepatocyte cell lines which were iron-loaded [71]. These findings support the results of the current study.

In conclusion, the results of this study show that increased levels of intracellular iron, in mouse primary hepatocytes *in vitro*, activated the Akt and AMPK pathways and resulted in decreased HGP. Insulin-induced activation of the Akt pathway was attenuated in these cells, possibly due

to decreased protein levels of IRS1/2 (Fig. 7). These findings may help explain why both insulin resistance and increased sensitivity have been observed in iron-overloaded states. They are of relevance to disease conditions characterized by hepatic iron overload such as hemochromatosis, thalassemia and non-alcoholic steatohepatitis, which are disorders known to be associated with increased risk of type 2 diabetes.

Author contributions

JV and JVJ performed all the experiments. ATM and SV critically analyzed results and reviewed the manuscript. JV and MJ designed the study, analyzed data and wrote the manuscript.

Funding

This work was funded by an Early Career Fellowship awarded to JV by the Wellcome Trust-DBT India Alliance (Ref no. 500190/Z/11/Z) and by a Fluid Research Grant awarded to MJ by Christian Medical College, Vellore (IRB no. 8686 dated 26.02.2014).

Disclosure statement

The authors have no conflicts of interest to declare.

References

[1] J.A. Simcox, D.A. McClain, Iron and Diabetes Risk, Cell Metab. 17 (2013) 329–341. doi:10.1016/j.cmet.2013.02.007.

[2] P.A. Merkel, D.C. Simonson, S.A. Amiel, G. Plewe, R.S. Sherwin, H.A. Pearson, W.V. Tamborlane, Insulin resistance and hyperinsulinemia in patients with thalassemia major treated by hypertransfusion, N. Engl. J. Med. 318 (1988) 809–814. doi:10.1056/NEJM198803313181303.

[3] M.R. Gamberini, V. De Sanctis, G. Gilli, Hypogonadism, diabetes mellitus, hypothyroidism, hypoparathyroidism: incidence and prevalence related to iron overload and chelation therapy in patients with thalassaemia major followed from 1980 to 2007 in the Ferrara Centre, Pediatr. Endocrinol. Rev. PER. 6 Suppl 1 (2008) 158–169.

[4] J.M. Fernández-Real, G. Peñarroja, A. Castro, F. García-Bragado, I. Hernández-Aguado, W. Ricart, Blood letting in high-ferritin type 2 diabetes: effects on insulin sensitivity and beta-cell function, Diabetes. 51 (2002) 1000–1004.

[5] F.S. Facchini, Effect of phlebotomy on plasma glucose and insulin concentrations, Diabetes Care. 21 (1998) 2190.

[6] S.A. Henderson, P.R. Dallman, G.A. Brooks, Glucose turnover and oxidation are increased in the iron-deficient anemic rat, Am. J. Physiol. 250 (1986) E414-421.

[7] M.J. Borel, J.L. Beard, P.A. Farrell, Hepatic glucose production and insulin sensitivity and responsiveness in iron-deficient anemic rats, Am. J. Physiol. 264 (1993) E380-390.

[8] Y. Minamiyama, S. Takemura, S. Kodai, H. Shinkawa, T. Tsukioka, H. Ichikawa, Y. Naito, T. Yoshikawa, S. Okada, Iron restriction improves type 2 diabetes mellitus in Otsuka Long-Evans Tokushima fatty rats, Am. J. Physiol. - Endocrinol. Metab. 298 (2010) E1140–E1149. doi:10.1152/ajpendo.00620.2009.

[9] R.C. Cooksey, D. Jones, S. Gabrielsen, J. Huang, J.A. Simcox, B. Luo, Y. Soesanto, H. Rienhoff, E.D. Abel, D.A. McClain, Dietary iron restriction or iron chelation protects from diabetes and loss of beta-cell function in the obese (ob/ob lep-/-) mouse, Am. J. Physiol. Endocrinol. Metab. 298 (2010) E1236-1243. doi:10.1152/ajpendo.00022.2010.

[10] P. Dongiovanni, L. Valenti, A. Ludovica Fracanzani, S. Gatti, G. Cairo, S. Fargion, Iron depletion by deferoxamine up-regulates glucose uptake and insulin signaling in hepatoma cells and in rat liver, Am. J. Pathol. 172 (2008) 738–747. doi:10.2353/ajpath.2008.070097.

[11] P. Dongiovanni, M. Ruscica, R. Rametta, S. Recalcati, L. Steffani, S. Gatti, D. Girelli, G. Cairo, P. Magni, S. Fargion, L. Valenti, Dietary iron overload induces visceral adipose tissue insulin resistance, Am. J. Pathol. 182 (2013) 2254–2263. doi:10.1016/j.ajpath.2013.02.019.

[12] R.A. Rizza, Pathogenesis of fasting and postprandial hyperglycemia in type 2 diabetes: implications for therapy, Diabetes. 59 (2010) 2697–2707. doi:10.2337/db10-1032.

[13] H.V. Lin, D. Accili, Hormonal regulation of hepatic glucose production in health and disease, Cell Metab. 14 (2011) 9–19. doi:10.1016/j.cmet.2011.06.003.

[14] R. Bartrons, L. Hue, E. Van Schaftingen, H.G. Hers, Hormonal control of fructose 2,6-bisphosphate concentration in isolated rat hepatocytes., Biochem. J. 214 (1983) 829–837.

[15] E. Van Schaftingen, D.R. Davies, H.-G. Hers, Inactivation of phosphofructokinase 2 by cyclic AMP-dependent protein kinase, Biochem. Biophys. Res. Commun. 103 (1981) 362–368. doi:10.1016/0006-291X(81)91701-0.

[16] G. Jiang, B.B. Zhang, Glucagon and regulation of glucose metabolism, Am. J. Physiol. Endocrinol. Metab. 284 (2003) E671-678. doi:10.1152/ajpendo.00492.2002.

[17] A.D. Cherrington, Banting Lecture 1997. Control of glucose uptake and release by the liver in vivo, Diabetes. 48 (1999) 1198–1214.

[18] D.R. Alessi, M. Andjelkovic, B. Caudwell, P. Cron, N. Morrice, P. Cohen, B.A. Hemmings, Mechanism of activation of protein kinase B by insulin and IGF-1., EMBO J. 15 (1996) 6541–6551.
[19] B.D. Manning, L.C. Cantley, AKT/PKB signaling: navigating downstream, Cell. 129 (2007) 1261–1274. doi:10.1016/j.cell.2007.06.009.
[20] P.M. Titchenell, Q. Chu, B.R. Monks, M.J. Birnbaum, Hepatic insulin signalling is dispensable for suppression of glucose output by insulin in vivo, Nat. Commun. 6 (2015) 7078. doi:10.1038/ncomms8078.
[21] D.G. Hardie, F.A. Ross, S.A. Hawley, AMPK: a nutrient and energy sensor that maintains energy homeostasis, Nat. Rev. Mol. Cell Biol. 13 (2012) 251–262. doi:10.1038/nrm3311.
[22] J.-M. Lee, W.-Y. Seo, K.-H. Song, D. Chanda, Y.D. Kim, D.-K. Kim, M.-W. Lee, D. Ryu, Y.-H. Kim, J.-R. Noh, C.-H. Lee, J.Y.L. Chiang, S.-H. Koo, H.-S. Choi, AMPK-dependent repression of hepatic gluconeogenesis via disruption of CREB.CRTC2 complex by orphan nuclear receptor small heterodimer partner, J. Biol. Chem. 285 (2010) 32182–32191. doi:10.1074/jbc.M110.134890.
[23] M. Johanns, Y.-C. Lai, M.-F. Hsu, R. Jacobs, D. Vertommen, J. Van Sande, J.E. Dumont, A. Woods, D. Carling, L. Hue, B. Viollet, M. Foretz, M.H. Rider, AMPK antagonizes hepatic glucagon-stimulated cyclic AMP signalling via phosphorylation-induced activation of cyclic nucleotide phosphodiesterase 4B, Nat. Commun. 7 (2016) 10856. doi:10.1038/ncomms10856.
[24] A. Pietrangelo, Hereditary hemochromatosis--a new look at an old disease, N. Engl. J. Med. 350 (2004) 2383–2397. doi:10.1056/NEJMra031573.
[25] J. Huang, J.S. Gabrielsen, R.C. Cooksey, B. Luo, L.G. Boros, D.L. Jones, H.A. Jouihan, Y. Soesanto, L. Knecht, M.W. Hazel, J.P. Kushner, D.A. McClain, Increased glucose disposal and AMP-dependent kinase signaling in a mouse model of hemochromatosis, J. Biol. Chem. 282 (2007) 37501–37507. doi:10.1074/jbc.M703625200.
[26] D.A. McClain, D. Abraham, J. Rogers, R. Brady, P. Gault, R. Ajioka, J.P. Kushner, High prevalence of abnormal glucose homeostasis secondary to decreased insulin secretion in individuals with hereditary haemochromatosis, Diabetologia. 49 (2006) 1661–1669. doi:10.1007/s00125-006-0200-0.
[27] P. Brissot, T.L. Wright, W.L. Ma, R.A. Weisiger, Efficient clearance of non-transferrin-bound iron by rat liver. Implications for hepatic iron loading in iron overload states., J. Clin. Invest. 76 (1985) 1463–1470. doi:10.1172/JCI112125.
[28] X. Wang, X. Fang, F. Wang, Pleiotropic actions of iron balance in diabetes mellitus, Rev. Endocr. Metab. Disord. 16 (2015) 15–23. doi:10.1007/s11154-014-9303-y.
[29] J. Huang, J. Simcox, T.C. Mitchell, D. Jones, J. Cox, B. Luo, R.C. Cooksey, L.G. Boros, D.A. McClain, Iron regulates glucose homeostasis in liver and muscle via AMP-activated protein kinase in mice, FASEB J. Off. Publ. Fed. Am. Soc. Exp. Biol. 27 (2013) 2845–2854. doi:10.1096/fj.12-216929.
[30] W. Zhang, R.M. Sargis, P.A. Volden, C.M. Carmean, X.J. Sun, M.J. Brady, PCB 126 and other dioxin-like PCBs specifically suppress hepatic PEPCK expression via the aryl hydrocarbon receptor, PloS One. 7 (2012) e37103. doi:10.1371/journal.pone.0037103.
[31] S. Silva-Gomes, A.G. Santos, C. Caldas, C.M. Silva, J.V. Neves, J. Lopes, F. Carneiro, P.N. Rodrigues, T.L. Duarte, Transcription factor NRF2 protects mice against dietary iron-induced liver injury by preventing hepatocytic cell death, J. Hepatol. 60 (2014) 354–361. doi:10.1016/j.jhep.2013.09.004.
[32] R. Enat, D.M. Jefferson, N. Ruiz-Opazo, Z. Gatmaitan, L.A. Leinwand, L.M. Reid, Hepatocyte proliferation in vitro: its dependence on the use of serum-free hormonally defined medium and substrata of extracellular matrix, Proc. Natl. Acad. Sci. 81 (1984) 1411–1415.
[33] R.H. Burdon, P.H. van Knippenberg, eds., Chapter 11 Monolayer culture of hepatocytes, in: Lab. Tech. Biochem. Mol. Biol., Elsevier, 1991: pp. 265–354. doi:10.1016/S0075-7535(08)70032-9.

[34] P. Puigserver, J. Rhee, J. Donovan, C.J. Walkey, J.C. Yoon, F. Oriente, Y. Kitamura, J. Altomonte, H. Dong, D. Accili, B.M. Spiegelman, Insulin-regulated hepatic gluconeogenesis through FOXO1–PGC-1α interaction, Nature. 423 (2003) 550–555. doi:10.1038/nature01667.

[35] R. Dentin, Y. Liu, S.-H. Koo, S. Hedrick, T. Vargas, J. Heredia, J.Y. Iii, M. Montminy, Insulin modulates gluconeogenesis by inhibition of the coactivator TORC2, Nature. 449 (2007) 366. doi:10.1038/nature06128.

[36] J.R. Cook, F. Langlet, Y. Kido, D. Accili, Pathogenesis of selective insulin resistance in isolated hepatocytes, J. Biol. Chem. 290 (2015) 13972–13980. doi:10.1074/jbc.M115.638197.

[37] Z.I. Cabantchik, Labile iron in cells and body fluids: physiology, pathology, and pharmacology, Front. Pharmacol. 5 (2014) 45. doi:10.3389/fphar.2014.00045.

[38] J. Varghese, J.V. James, S. Sagi, S. Chakraborty, A. Sukumaran, B. Ramakrishna, M. Jacob, Decreased hepatic iron in response to alcohol may contribute to alcohol-induced suppression of hepcidin, Br. J. Nutr. 115 (2016) 1978–1986. doi:10.1017/S0007114516001197.

[39] J.D. Torrance, T.H. Bothwell, A simple technique for measuring storage iron concentrations in formalinised liver samples, S. Afr. J. Med. Sci. 33 (1968) 9–11.

[40] F. Rajas, N. Bruni, S. Montano, C. Zitoun, G. Mithieux, The glucose-6 phosphatase gene is expressed in human and rat small intestine: regulation of expression in fasted and diabetic rats, Gastroenterology. 117 (1999) 132–139.

[41] H.H. Taussky, E. Shorr, W. the technical assistance of G. Kurzmann, A Microcolorimetric Method for the Determination of Inorganic Phosphorus, J. Biol. Chem. 202 (1953) 675–685.

[42] A.E. Harper, Glucose-6-phosphatase, in: Methods Enzym. Anal., Elsevier, 1965: pp. 788–792.

[43] N. Horike, H. Sakoda, A. Kushiyama, H. Ono, M. Fujishiro, H. Kamata, K. Nishiyama, Y. Uchijima, Y. Kurihara, H. Kurihara, T. Asano, AMP-activated protein kinase activation increases phosphorylation of glycogen synthase kinase 3beta and thereby reduces cAMP-responsive element transcriptional activity and phosphoenolpyruvate carboxykinase C gene expression in the liver, J. Biol. Chem. 283 (2008) 33902–33910. doi:10.1074/jbc.M802537200.

[44] J.D. Horton, J.L. Goldstein, M.S. Brown, SREBPs: activators of the complete program of cholesterol and fatty acid synthesis in the liver, J. Clin. Invest. 109 (2002) 1125–1131. doi:10.1172/JCI15593.

[45] Y. Li, S. Xu, M.M. Mihaylova, B. Zheng, X. Hou, B. Jiang, O. Park, Z. Luo, E. Lefai, J.Y.-J. Shyy, B. Gao, M. Wierzbicki, T.J. Verbeuren, R.J. Shaw, R.A. Cohen, M. Zang, AMPK phosphorylates and inhibits SREBP activity to attenuate hepatic steatosis and atherosclerosis in diet-induced insulin-resistant mice, Cell Metab. 13 (2011) 376–388. doi:10.1016/j.cmet.2011.03.009.

[46] T. Ide, H. Shimano, N. Yahagi, T. Matsuzaka, M. Nakakuki, T. Yamamoto, Y. Nakagawa, A. Takahashi, H. Suzuki, H. Sone, H. Toyoshima, A. Fukamizu, N. Yamada, SREBPs suppress IRS-2-mediated insulin signalling in the liver, Nat. Cell Biol. 6 (2004) 351–357. doi:10.1038/ncb1111.

[47] K.B. Seamon, J.W. Daly, Forskolin: its biological and chemical properties, Adv. Cyclic Nucleotide Protein Phosphorylation Res. 20 (1986) 1–150.

[48] E. Baker, S.M. Baker, E.H. Morgan, Characterisation of non-transferrin-bound iron (ferric citrate) uptake by rat hepatocytes in culture, Biochim. Biophys. Acta. 1380 (1998) 21–30.

[49] R.W. Evans, R. Rafique, A. Zarea, C. Rapisarda, R. Cammack, P.J. Evans, J.B. Porter, R.C. Hider, Nature of non-transferrin-bound iron: studies on iron citrate complexes and thalassemic sera, J. Biol. Inorg. Chem. JBIC Publ. Soc. Biol. Inorg. Chem. 13 (2008) 57–74. doi:10.1007/s00775-007-0297-8.

[50] I. Chopra, H.F. Li, H. Wang, K.A. Webster, Phosphorylation of the insulin receptor by AMP-activated protein kinase (AMPK) promotes ligand-independent activation of the insulin signalling pathway in rodent muscle, Diabetologia. 55 (2012) 783–794. doi:10.1007/s00125-011-2407-y.

[51] T. Zheng, X. Yang, D. Wu, S. Xing, F. Bian, W. Li, J. Chi, X. Bai, G. Wu, X. Chen, Y. Zhang, S. Jin, Salidroside ameliorates insulin resistance through activation of a mitochondria-associated AMPK/PI3K/Akt/GSK3β pathway, Br. J. Pharmacol. 172 (2015) 3284–3301. doi:10.1111/bph.13120.

[52] S. Krishan, D.R. Richardson, S. Sahni, The Anticancer Agent, Di-2-Pyridylketone 4,4-Dimethyl-3-Thiosemicarbazone (Dp44mT), Up-Regulates the AMPK-Dependent Energy Homeostasis Pathway in Cancer Cells, Biochim. Biophys. Acta BBA - Mol. Cell Res. 1863 (2016) 2916–2933. doi:10.1016/j.bbamcr.2016.09.011.

[53] H. Lodish, A. Berk, S.L. Zipursky, P. Matsudaira, D. Baltimore, J. Darnell, Electron Transport and Oxidative Phosphorylation, (2000). https://www.ncbi.nlm.nih.gov/books/NBK21528/ (accessed May 16, 2018).

[54] J. Nakae, T. Kitamura, D.L. Silver, D. Accili, The forkhead transcription factor Foxo1 (Fkhr) confers insulin sensitivity onto glucose-6-phosphatase expression, J. Clin. Invest. 108 (2001) 1359–1367.

[55] D. Schmoll, K.S. Walker, D.R. Alessi, R. Grempler, A. Burchell, S. Guo, R. Walther, T.G. Unterman, Regulation of glucose-6-phosphatase gene expression by protein kinase Balpha and the forkhead transcription factor FKHR. Evidence for insulin response unit-dependent and -independent effects of insulin on promoter activity, J. Biol. Chem. 275 (2000) 36324–36333. doi:10.1074/jbc.M003616200.

[56] L. Agius, Glucokinase and molecular aspects of liver glycogen metabolism, Biochem. J. 414 (2008) 1–18. doi:10.1042/BJ20080595.

[57] M.L. Massa, J.J. Gagliardino, F. Francini, Liver glucokinase: An overview on the regulatory mechanisms of its activity, IUBMB Life. 63 (2011) 1–6. doi:10.1002/iub.411.

[58] J.M. Berg, J.L. Tymoczko, L. Stryer, The Glycolytic Pathway Is Tightly Controlled, (2002). https://www.ncbi.nlm.nih.gov/books/NBK22395/ (accessed May 16, 2018).

[59] S.J. Pilkis, T.H. Claus, Hepatic gluconeogenesis/glycolysis: regulation and structure/function relationships of substrate cycle enzymes, Annu. Rev. Nutr. 11 (1991) 465–515. doi:10.1146/annurev.nu.11.070191.002341.

[60] H.J. Lee, J.S. Choi, H.J. Lee, W.-H. Kim, S.I. Park, J. Song, Effect of excess iron on oxidative stress and gluconeogenesis through hepcidin during mitochondrial dysfunction, J. Nutr. Biochem. 26 (2015) 1414–1423. doi:10.1016/j.jnutbio.2015.07.008.

[61] P.M. Titchenell, W.J. Quinn, M. Lu, Q. Chu, W. Lu, C. Li, H. Chen, B.R. Monks, J. Chen, J.D. Rabinowitz, M.J. Birnbaum, Direct Hepatocyte Insulin Signaling Is Required for Lipogenesis but Is Dispensable for the Suppression of Glucose Production, Cell Metab. 23 (2016) 1154–1166. doi:10.1016/j.cmet.2016.04.022.

[62] R.J. Perry, J.-P.G. Camporez, R. Kursawe, P.M. Titchenell, D. Zhang, C.J. Perry, M.J. Jurczak, A. Abudukadier, M.S. Han, X.-M. Zhang, H.-B. Ruan, X. Yang, S. Caprio, S.M. Kaech, H.S. Sul, M.J. Birnbaum, R.J. Davis, G.W. Cline, K.F. Petersen, G.I. Shulman, Hepatic acetyl CoA links adipose tissue inflammation to hepatic insulin resistance and type 2 diabetes, Cell. 160 (2015) 745–758. doi:10.1016/j.cell.2015.01.012.

[63] V. Aguirre, E.D. Werner, J. Giraud, Y.H. Lee, S.E. Shoelson, M.F. White, Phosphorylation of Ser307 in insulin receptor substrate-1 blocks interactions with the insulin receptor and inhibits insulin action, J. Biol. Chem. 277 (2002) 1531–1537. doi:10.1074/jbc.M101521200.

[64] V. Aguirre, T. Uchida, L. Yenush, R. Davis, M.F. White, The c-Jun NH(2)-terminal kinase promotes insulin resistance during association with insulin receptor substrate-1 and phosphorylation of Ser(307), J. Biol. Chem. 275 (2000) 9047–9054.

[65] C.J. Carlson, M.F. White, C.M. Rondinone, Mammalian target of rapamycin regulates IRS-1 serine 307 phosphorylation, Biochem. Biophys. Res. Commun. 316 (2004) 533–539. doi:10.1016/j.bbrc.2004.02.082.

[66] L.-Y. Qiao, R. Zhande, T.L. Jetton, G. Zhou, X.J. Sun, In vivo phosphorylation of insulin receptor substrate 1 at serine 789 by a novel serine kinase in insulin-resistant rodents, J. Biol. Chem. 277 (2002) 26530–26539. doi:10.1074/jbc.M201494200.

[67] K.E. Brown, M.M. Mathahs, K.A. Broadhurst, J. Weydert, Chronic iron overload stimulates hepatocyte proliferation and cyclin D1 expression in rodent liver, Transl. Res. J. Lab. Clin. Med. 148 (2006) 55–62. doi:10.1016/j.trsl.2006.03.002.

[68] M. Li, Y. Tang, L. Wu, F. Mo, X. Wang, H. Li, R. Qi, H. Zhang, A. Srivastava, C. Ling, The hepatocyte-specific HNF4α/miR-122 pathway contributes to iron overload–mediated hepatic inflammation, Blood. 130 (2017) 1041–1051. doi:10.1182/blood-2016-12-755967.

[69] T. Matsui, T. Nagoshi, E.-G. Hong, I. Luptak, K. Hartil, L. Li, N. Gorovits, M.J. Charron, J.K. Kim, R. Tian, A. Rosenzweig, Effects of chronic Akt activation on glucose uptake in the heart, Am. J. Physiol. Endocrinol. Metab. 290 (2006) E789-797. doi:10.1152/ajpendo.00564.2004.

[70] Y.G. Ni, N. Wang, D.J. Cao, N. Sachan, D.J. Morris, R.D. Gerard, M. Kuro-O, B.A. Rothermel, J.A. Hill, FoxO transcription factors activate Akt and attenuate insulin signaling in heart by inhibiting protein phosphatases, Proc. Natl. Acad. Sci. U. S. A. 104 (2007) 20517–20522. doi:10.1073/pnas.0610290104.

[71] D.J. Messner, B.H. Rhieu, K.V. Kowdley, Iron overload causes oxidative stress and impaired insulin signaling in AML-12 hepatocytes, Dig. Dis. Sci. 58 (2013) 1899–1908. doi:10.1007/s10620-013-2648-3.

Figure legends

Fig. 1: Treatment of hepatocytes with FAC increased intracellular iron content

A: Intracellular iron levels estimated using a bathophenanthrolene-based colorimetric assay.

B and C: Representative images and densitometric quantification of western blots for ferritin (light chain) (B) and TfR1 (C). Bands obtained for β-actin are shown as loading controls.

D: Representative fluorescent microscopic images showing quenching of calcein fluorescence by treatment with FAC. Images shown in 10x magnification.

E and F: Determination of cell viability by MTT assays (E) and estimation of LDH activity in the medium (F) following treatment of cells with FAC.

Data represent mean ± SD of results obtained from at least three independent experiments (primary hepatocytes isolated from at least 3 different mice), with each incubation done in duplicate or triplicate, under the specified conditions. Dissimilar alphabets against bars in each panel indicate data that are significantly different from one another. A p value <0.05 was taken to indicate statistical significance in all cases.

Figure 2: Treatment with iron increased phosphorylation of Akt and its downstream targets, Gsk3β and FoxO1

A-D: Mouse primary hepatocytes were treated with FAC at various concentrations (as indicated) for 16 hours. Representative images for western blots and densitometric quantification of the bands obtained are shown for p-Akt [Thr308]/Akt (A), p-Akt [Ser473]/Akt (B), p-Gsk3β [Ser9]/ Gsk3β (C) and p-FoxO1 [Ser256]/FoxO1 (D). Bands obtained for β-actin are shown as loading controls.

E and F: Hepatocytes treated with FAC (75 μM) for 16 hours were washed and further treated with DFO (250 μM) for 6 hours. Intracellular iron content (E) estimated at the end of the incubation periods and representative images and densitometric quantification of the bands for pAkt (Ser473)/Akt (F) are shown. Bands obtained for β-actin are shown as loading controls.

Data represent mean ± SD of results obtained from at least three independent experiments (primary hepatocytes isolated from at least 3 different mice), with each incubation done in duplicate or triplicate, under the specified conditions. Dissimilar alphabets against bars in each panel indicate data that are significantly different from one another. A p value <0.05 was taken to indicate statistical significance in all cases. In panel F, * indicates p <0.05.

Figure 3: Treatment with iron activated AMP-activated kinase (AMPK)

A: Representative images of western blots for p-AMPK (Thr172)/AMPK and p-ACC (Ser79)/ACC and densitometric quantification of bands obtained for p-AMPK (Thr172)/AMPK are shown. Bands obtained for β-actin are shown as loading controls.

B-E: Gene expression (determined by qPCR) of acetyl CoA carboxylase (*Acaca*) (B), fatty acid synthase (*Fasn*) (C), IRS-2 (*Irs2*) (D) and IRS-1 (*Irs1*) (E).

Data represent mean ± SD of results obtained from at least three independent experiments (primary hepatocytes isolated from at least 3 different mice), with each incubation done in duplicate or triplicate, under the specified conditions. Dissimilar alphabets against bars in each panel indicate data that are significantly different from one another. A p value <0.05 was taken to indicate statistical significance in all cases.

Figure 4: Treatment with iron decreased hepatocyte glucose production (HGP)

A and B: HGP assay using lactate as the gluconeogenic substrate in the presence (B) or absence (A) of forskolin (25μM) for 3 h.

C and D: HGP assay using glycerol as the gluconeogenic substrate in the presence (D) or absence (C) of forskolin (25μM) for 3 h.

E and F: Gene expression (determined by qPCR) of *G6pc* (E) and G6Pase enzyme activity (F) in the presence and absence of forskolin (25 μM) for 3 h.

Data represent mean ± SD of results obtained from at least three independent experiments (primary hepatocytes isolated from at least 3 different mice), with each incubation done in duplicate or triplicate, under the specified conditions. In A-D, * indicates p<0.05 compared to FAC at 0 μM and # indicates p<0.05 when compared to FAC at 7.5 μM. In E and F, dissimilar alphabets against bars in each panel indicate data that are significantly different from one another. A p value <0.05 was taken to indicate statistical significance in all cases.

Figure 5: Treatment with iron rendered hepatocytes less sensitive to insulin-induced activation of the Akt pathway

A and B: Hepatocytes were treated with FAC at various concentrations (as indicated) for 16 hours and then treated with insulin (10 nM) or normal saline for 5 min. The effect of insulin treatment on phosphorylation of Akt (A) or Gsk3β (B) was determined as a ratio of p-Akt or p-GSK3β levels in the presence of insulin to that in its absence. Bands obtained for β-actin are shown as loading controls.

C, D and E: Hepatocytes were treated with FAC at various concentrations (as indicated) for 16 hours and then treated with insulin (10 nM) or normal saline for 3 hours. Gene expression of *G6pc* (C) and *Gck* (E) (determined by qPCR) and G6Pase enzyme activity (D) are shown.

Data represent mean ± SD of results obtained from at least three independent experiments (primary hepatocytes isolated from at least 3 different mice), with each incubation done in duplicate or triplicate, under the specified conditions. Dissimilar alphabets against bars in each panel indicate data that are significantly different from one another. A p value of less than 0.05 was taken to indicate statistical significance in all cases.

Figure 6: Iron down-regulated protein levels of IRS1 and IRS2

Representative images and densitometric quantification of western blots for IRS1 (A), IRS2 (B), p-IRS1 (Ser307)/total IRS1 (C), p-IRS1 (Ser789)/total IRS1 (D) and p-JNK (E) are shown. Bands obtained for β-actin are shown as loading controls.

Data represent mean ± SD of results obtained from at least three independent experiments (primary hepatocytes isolated from at least 3 different mice), with each incubation done in duplicate, under the specified conditions. Dissimilar alphabets against bars in each panel indicate data that are significantly different from one another. A p value of less than 0.05 was taken to indicate statistical significance in all cases.

Figure 7: Schematic diagram of the proposed effect of intracellular iron on insulin signaling

Increased intracellular iron activated the Akt and AMPK pathways, resulting in decreased gluconeogenesis and hepatocyte glucose production. In addition, iron decreased levels of IRS-1 and 2, which are upstream of Akt in the insulin signaling pathway, resulting in decreased insulin-stimulated activation of the Akt pathway.

Table 1: Correlation analyses among parameters of interest in primary hepatocytes treated with iron

Sl. no	Parameter	Parameter	Spearman's correlation coefficient	p-value
1	Intracellular iron level vs.	p-Akt (Ser473)	0.648	0.004
		p-Akt (Thr308)	0.843	<0.001
		p-Gsk3β (Ser9)	0.771	0.003
		p-FoxO1 (Ser256)	0.652	0.008
		p-AMPK (Thr172)	0.812	<0.001
		p-IRS1 (Ser307)	0.470	0.049
		Total IRS1	- 0.667	0.002
		Total IRS2	- 0.684	0.007
2	p-Akt (Ser473) vs.	p-Akt (Thr308)	0.671	0.004
		p-Gsk3β (Ser9)	0.638	0.025
		p-FoxO1 (Ser256)	0.574	0.020
		p-AMPK (Thr172)	0.649	0.001
3	p-Akt (Thr308) vs.	p-Gsk3β (Ser9)	0.997	<0.001
		p-FoxO1 (Ser256)	0.641	0.007
		p-AMPK (Thr172)	0.747	0.001
4	p-Gsk3β (Ser9) vs.	p-FoxO1 (Ser256)	0.713	0.009
		p-AMPK (Thr172)	0.716	0.009
5	p-FoxO1 (Ser256) vs.	p-AMPK (Thr172)	0.515	0.041

Highlights

- Increased cellular iron levels activated Akt and AMPK signaling in hepatocytes.
- These effects were associated with decreased hepatic glucose production (HGP).
- Iron decreased insulin-induced activation of Akt and forskolin-induced HGP.
- Increased intracellular iron levels altered insulin sensitivity in hepatocytes.
- It caused basal activation of Akt and attenuation of insulin-induced activation.

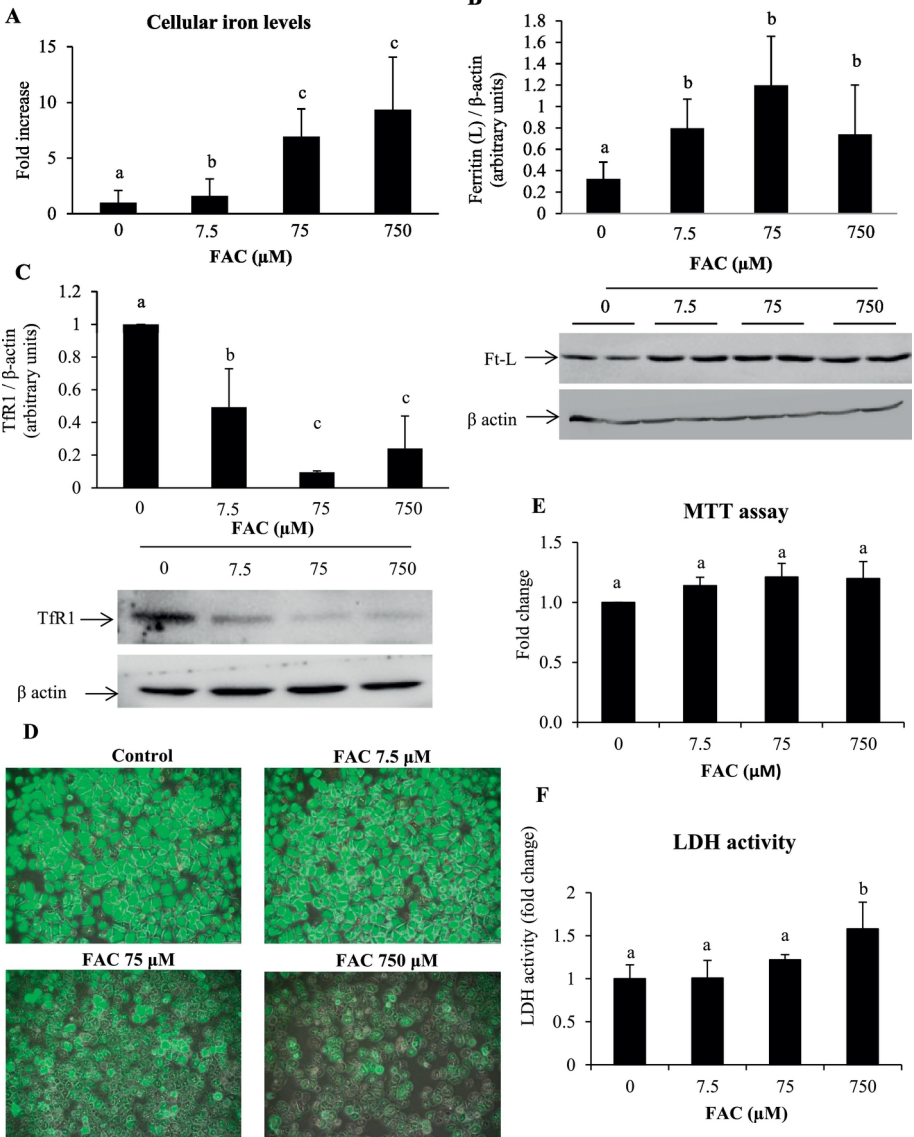
A
Cellular iron levels
Fold increase
15
10
5
0
a
b
c
c
0
7.5
75
750
FAC (μM)
B
Ferritin (L) / β-actin (arbitrary units)
1.8
1.6
1.4
1.2
1
0.8
0.6
0.4
0.2
0
a
b
b
b
0
7.5
75
750
FAC (μM)
C
TfR1 / β-actin (arbitrary units)
1.2
1
0.8
0.6
0.4
0.2
0
a
b
c
c
0
7.5
75
750
FAC (μM)
0
7.5
75
750
TfR1
β actin
0
7.5
75
750
Ft-L
β actin
D
Control
FAC 7.5 μM
FAC 75 μM
FAC 750 μM
E
MTT assay
Fold change
1.5
1.0
0.5
0.0
a
a
a
a
0
7.5
75
750
FAC (μM)
F
LDH activity
LDH activity (fold change)
2
1.5
1
0.5
0
a
a
a
b
0
7.5
75
750
FAC (μM)

Figure 1

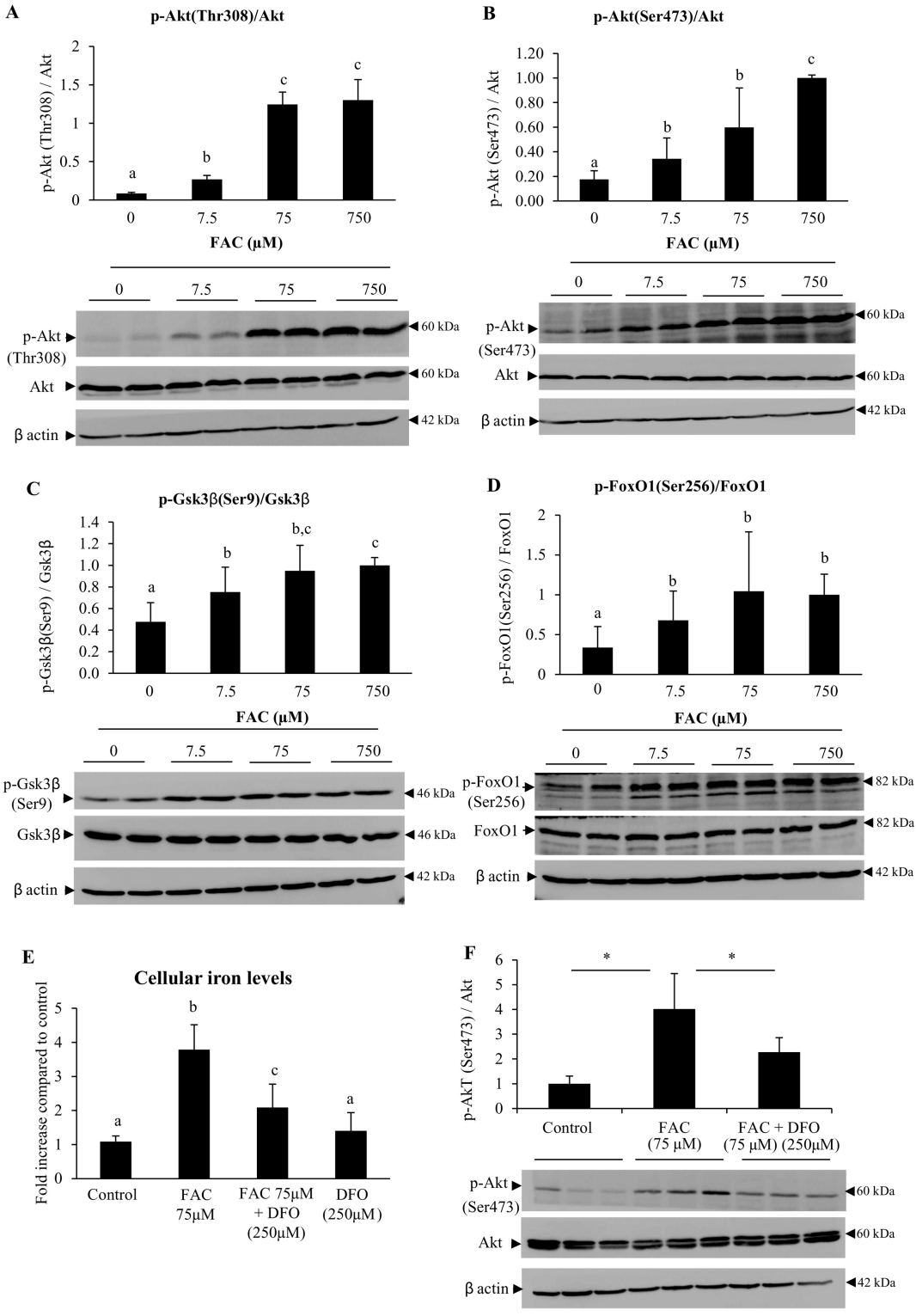
A
p-Akt(Thr308)/Akt
p-Akt (Thr308) / Akt
FAC (μM)
0
7.5
75
750
p-Akt (Thr308)
Akt
β actin
60 kDa
42 kDa
B
p-Akt(Ser473)/Akt
p-Akt (Ser473) / Akt
p-Akt (Ser473)
C
p-Gsk3β(Ser9)/Gsk3β
p-Gsk3β(Ser9) / Gsk3β
p-Gsk3β (Ser9)
Gsk3β
46 kDa
D
p-FoxO1(Ser256)/FoxO1
p-FoxO1(Ser256) / FoxO1
p-FoxO1 (Ser256)
FoxO1
82 kDa
E
Cellular iron levels
Fold increase compared to control
Control
FAC 75μM
FAC 75μM + DFO (250μM)
DFO (250μM)
F
p-AkT (Ser473) / Akt
FAC (75 μM)
FAC + DFO (75 μM) (250μM)

Figure 2

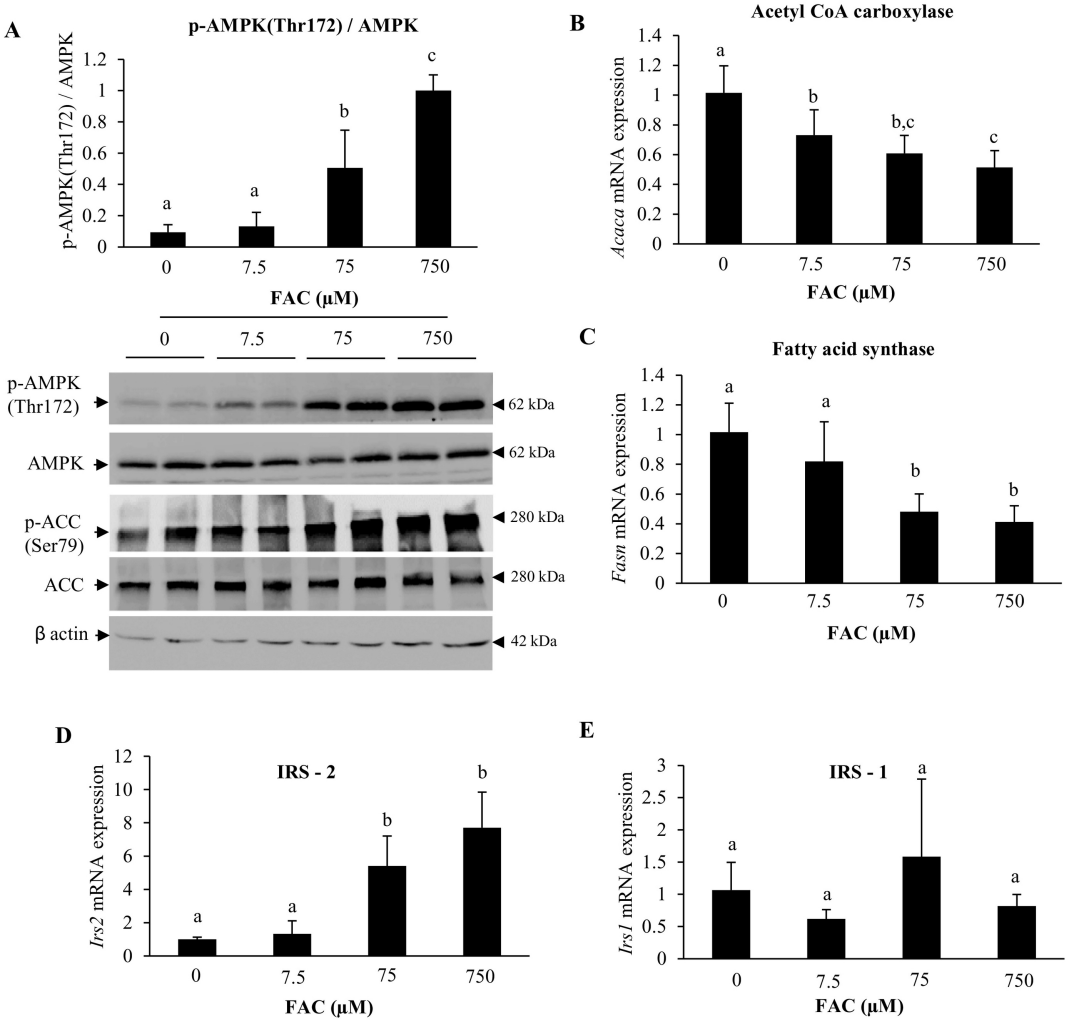
A
p-AMPK(Thr172) / AMPK
p-AMPK(Thr172) / AMPK
1.2
1
0.8
0.6
0.4
0.2
0
a
a
b
c
0
7.5
75
750
FAC (μM)
0
7.5
75
750
p-AMPK (Thr172)
AMPK
p-ACC (Ser79)
ACC
β actin
62 kDa
62 kDa
280 kDa
280 kDa
42 kDa
B
Acetyl CoA carboxylase
Acaca mRNA expression
1.4
1.2
1
0.8
0.6
0.4
0.2
0
a
b
b,c
c
0
7.5
75
750
FAC (μM)
C
Fatty acid synthase
Fasn mRNA expression
1.4
1.2
1
0.8
0.6
0.4
0.2
0
a
a
b
b
0
7.5
75
750
FAC (μM)
D
IRS - 2
Irs2 mRNA expression
12
10
8
6
4
2
0
a
a
b
b
0
7.5
75
750
FAC (μM)
E
IRS - 1
Irs1 mRNA expression
3
2.5
2
1.5
1
0.5
0
a
a
a
a
0
7.5
75
750
FAC (μM)

Figure 3

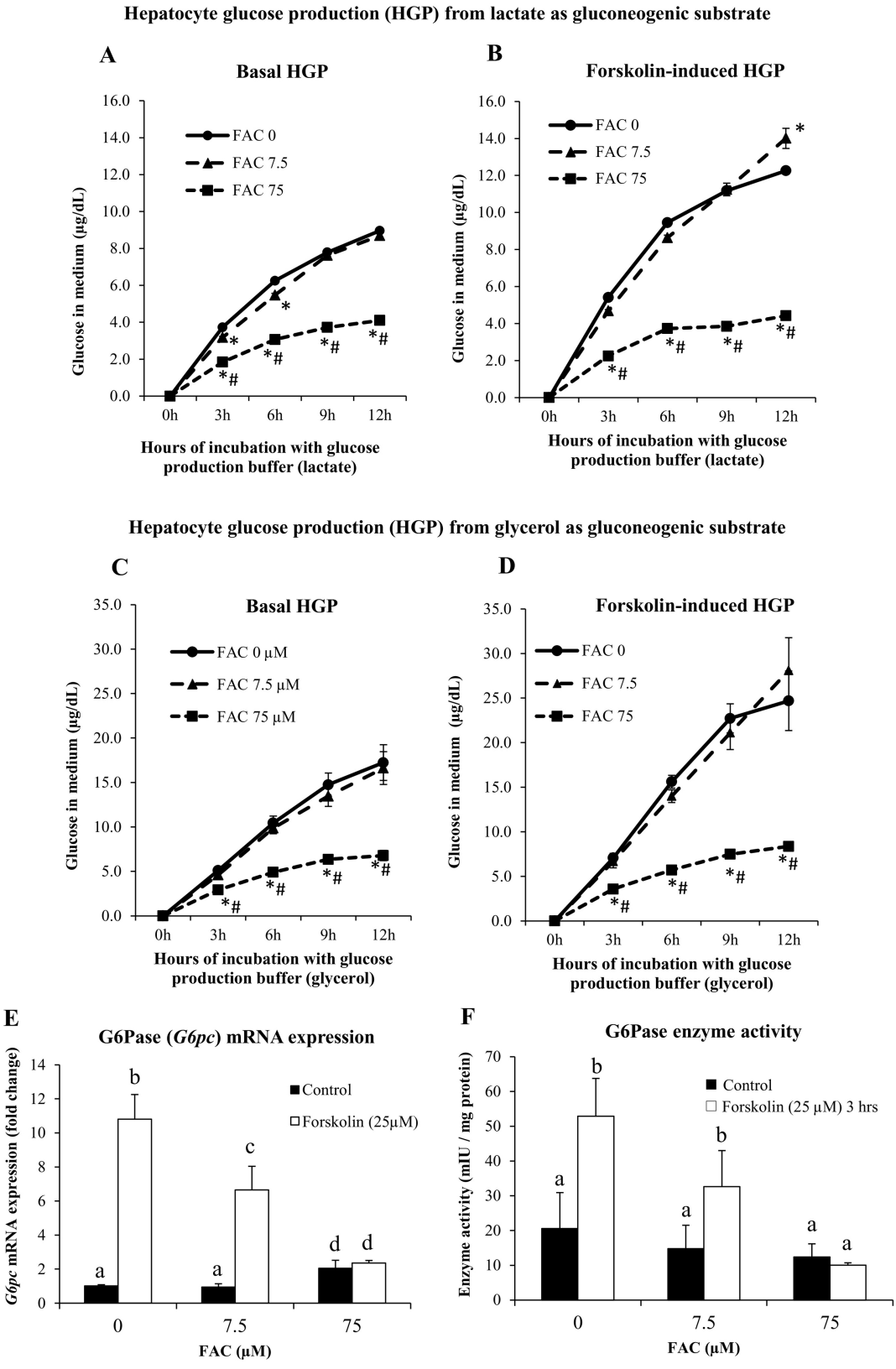
Hepatocyte glucose production (HGP) from lactate as gluconeogenic substrate
A
Basal HGP
Glucose in medium (µg/dL)
FAC 0
FAC 7.5
FAC 75
Hours of incubation with glucose production buffer (lactate)
B
Forskolin-induced HGP
Hepatocyte glucose production (HGP) from glycerol as gluconeogenic substrate
C
Basal HGP
FAC 0 µM
FAC 7.5 µM
FAC 75 µM
Hours of incubation with glucose production buffer (glycerol)
D
Forskolin-induced HGP
E
G6Pase (G6pc) mRNA expression
G6pc mRNA expression (fold change)
Control
Forskolin (25µM)
FAC (µM)
F
G6Pase enzyme activity
Enzyme activity (mIU / mg protein)
Forskolin (25 µM) 3 hrs

Figure 4

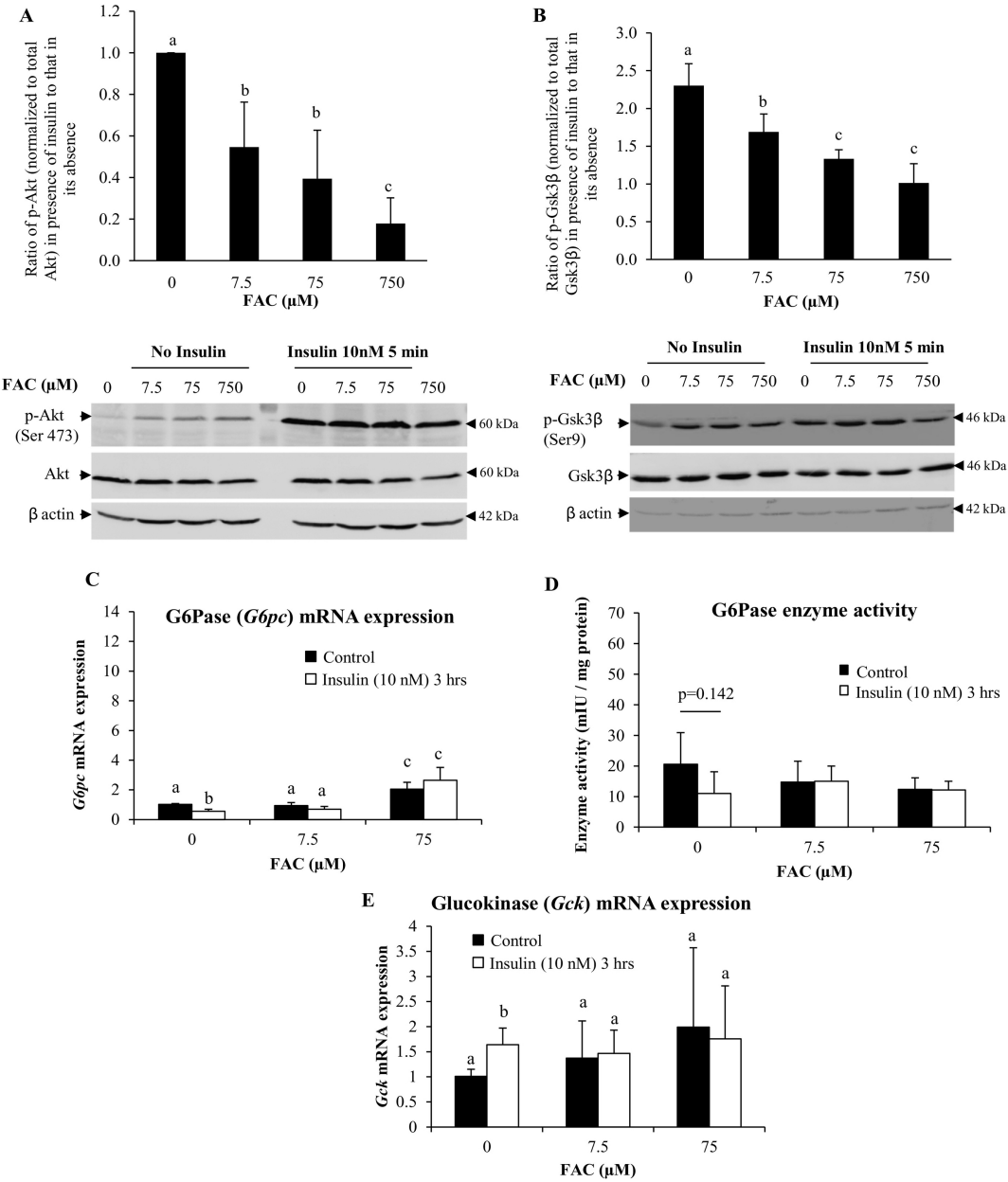
A
Ratio of p-Akt (normalized to total Akt) in presence of insulin to that in its absence
1.2
1.0
0.8
0.6
0.4
0.2
0.0
a
b
b
c
0
7.5
75
750
FAC (μM)
B
Ratio of p-Gsk3β (normalized to total Gsk3β) in presence of insulin to that in its absence
3.0
2.5
2.0
1.5
1.0
0.5
0.0
a
b
c
c
0
7.5
75
750
FAC (μM)
No Insulin
Insulin 10nM 5 min
FAC (μM) 0 7.5 75 750 0 7.5 75 750
p-Akt (Ser 473)
Akt
β actin
60 kDa
60 kDa
42 kDa
No Insulin
Insulin 10nM 5 min
FAC (μM) 0 7.5 75 750 0 7.5 75 750
p-Gsk3β (Ser9)
Gsk3β
β actin
46 kDa
46 kDa
42 kDa
C
G6Pase (G6pc) mRNA expression
G6pc mRNA expression
14
12
10
8
6
4
2
0
Control
Insulin (10 nM) 3 hrs
a
b
a
a
c
c
0
7.5
75
FAC (μM)
D
G6Pase enzyme activity
Enzyme activity (mIU / mg protein)
70
60
50
40
30
20
10
0
p=0.142
Control
Insulin (10 nM) 3 hrs
0
7.5
75
FAC (μM)
E
Glucokinase (Gck) mRNA expression
Gck mRNA expression
4
3.5
3
2.5
2
1.5
1
0.5
0
Control
Insulin (10 nM) 3 hrs
a
b
a
a
a
a
0
7.5
75
FAC (μM)

Figure 5

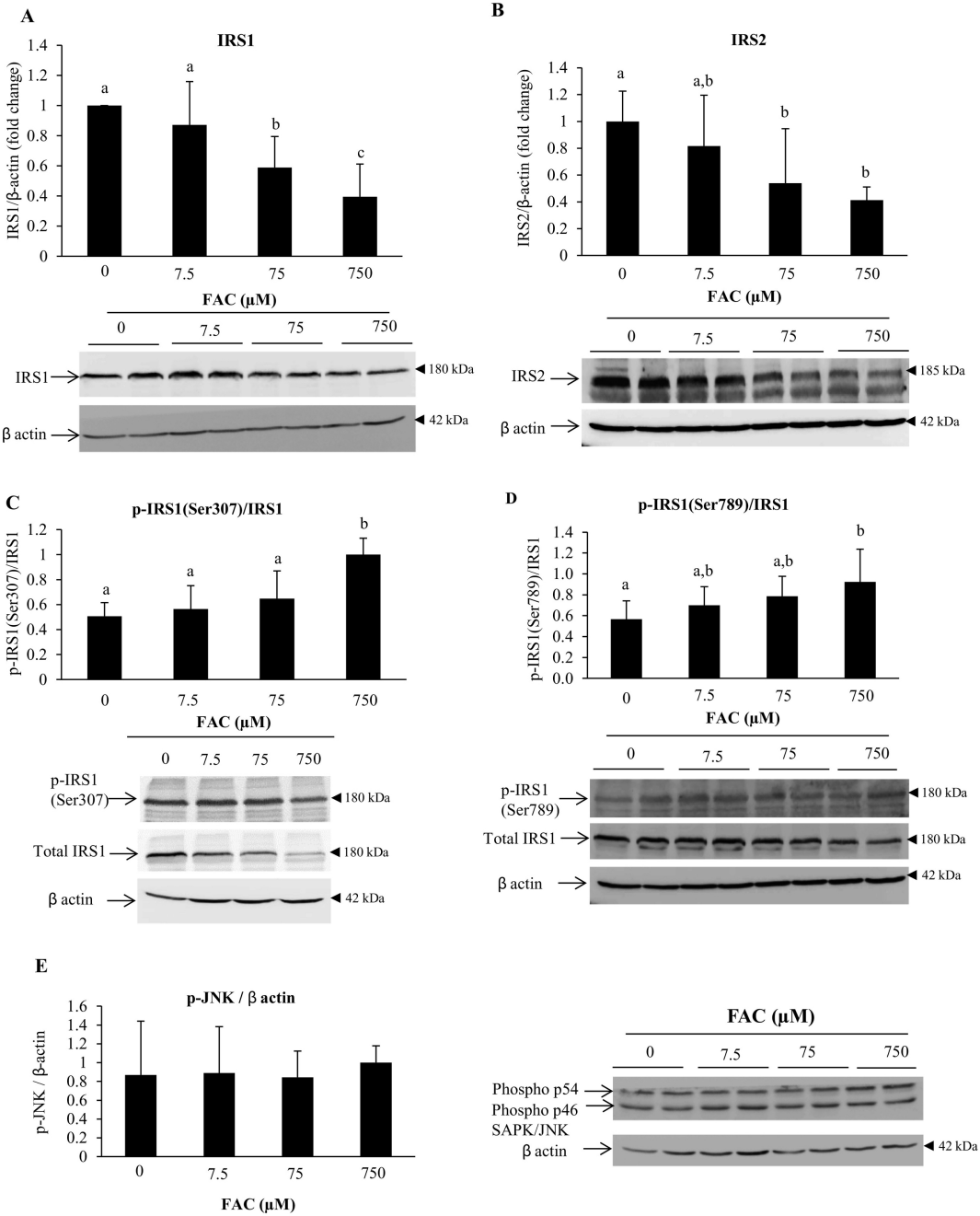
A
IRS1
IRS1/β-actin (fold change)
1.4
1.2
1
0.8
0.6
0.4
0.2
0
a
a
b
c
0
7.5
75
750
FAC (μM)
0
7.5
75
750
IRS1
180 kDa
β actin
42 kDa
B
IRS2
IRS2/β-actin (fold change)
a
a,b
b
b
0
7.5
75
750
FAC (μM)
0
7.5
75
750
IRS2
185 kDa
β actin
42 kDa
C
p-IRS1(Ser307)/IRS1
p-IRS1(Ser307)/IRS1
1.2
1
0.8
0.6
0.4
0.2
0
a
a
a
b
0
7.5
75
750
FAC (μM)
0
7.5
75
750
p-IRS1
(Ser307)
180 kDa
Total IRS1
180 kDa
β actin
42 kDa
D
p-IRS1(Ser789)/IRS1
p-IRS1(Ser789)/IRS1
1.4
1.2
1.0
0.8
0.6
0.4
0.2
0.0
a
a,b
a,b
b
0
7.5
75
750
FAC (μM)
0
7.5
75
750
p-IRS1
(Ser789)
180 kDa
Total IRS1
180 kDa
β actin
42 kDa
E
p-JNK / β actin
p-JNK / β-actin
1.6
1.4
1.2
1
0.8
0.6
0.4
0.2
0
0
7.5
75
750
FAC (μM)
FAC (μM)
0
7.5
75
750
Phospho p54
Phospho p46
SAPK/JNK
β actin
42 kDa

Figure 6

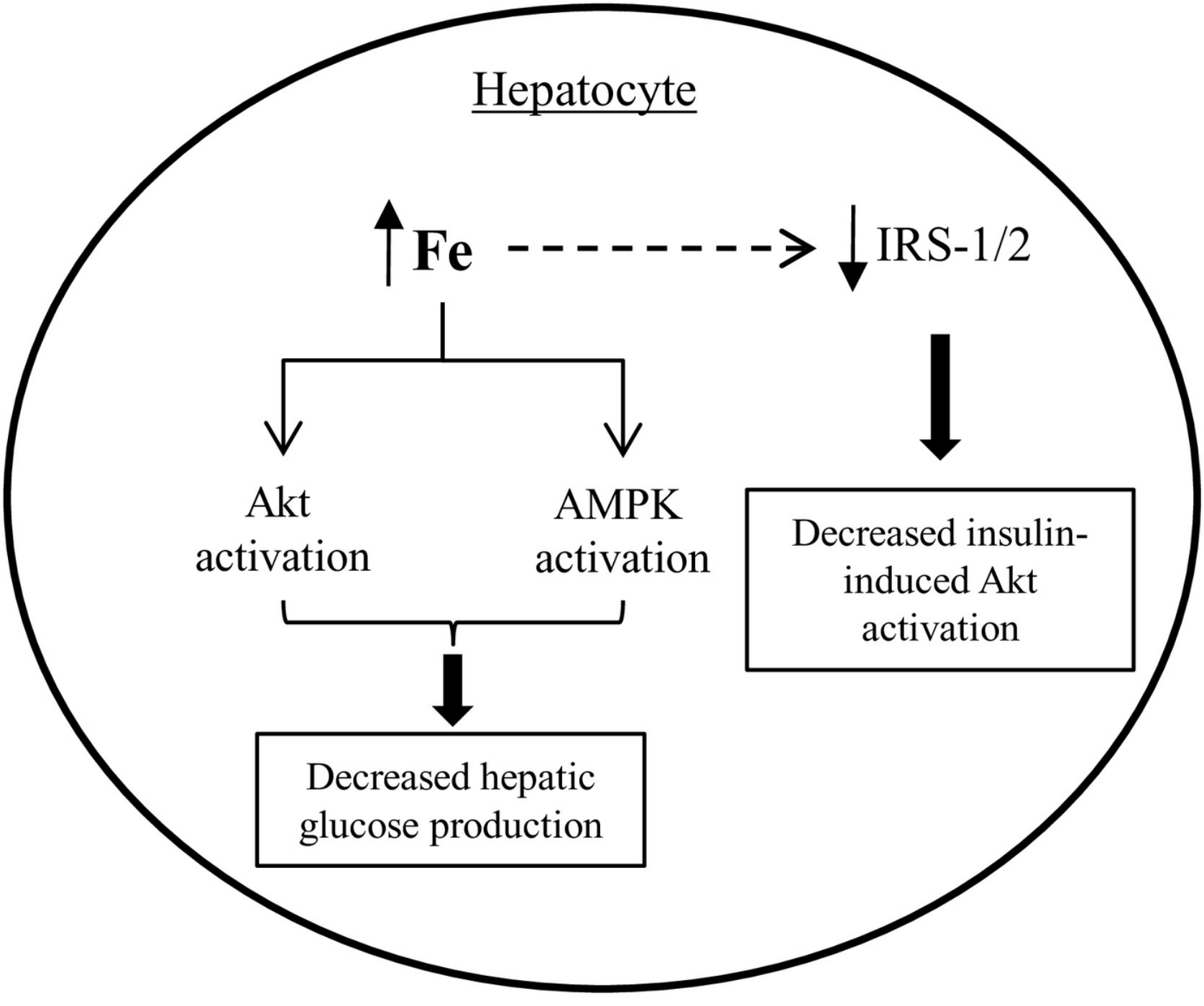
Hepatocyte
Fe
IRS-1/2
Akt activation
AMPK activation
Decreased insulin-induced Akt activation
Decreased hepatic glucose production

Figure 7